Article

Spatial Relationships between Pockmarks and Sub-Seabed Gas in Fjordic Settings: Evidence from Loch Linnhe, West Scotland

Allan Audsley [1,*], Tom Bradwell [1], John Howe [2] and John Baxter [3]

1   Department of Biological and Environmental Science, Faculty of Natural Sciences, University of Stirling, Stirling FK9 4LA, UK; tom.bradwell@stir.ac.uk
2   Scottish Association for Marine Science, Oban, Argyll PA37 1QA, UK; john.howe@sams.ac.uk
3   University of St Andrews, St Andrews KY16 9AJ, UK; john@oceanperspectives.com
*   Correspondence: ala2@stir.ac.uk

Abstract: Sub-seabed gas is commonly associated with seabed depressions known as pockmarks—the main venting sites for hydrocarbon gases to enter the water column. Sub-seabed gas accumulations are characterized by acoustically turbid or opaque zones in seismic reflection profiles, taking the form of gas blankets, curtains or plumes. How the migration of sub-seabed gas relates to the origin and distribution of pockmarks in nearshore and fjordic settings is not well understood. Using marine geophysical data from Loch Linnhe, a Scottish fjord, we show that shallow sub-seabed gas occurs predominantly within glaciomarine facies either as widespread blankets in basins or as isolated pockets. We use geospatial 'hot-spot' analysis conducted in ArcGIS to identify clusters of pockmarks and acoustic (sub-seabed) profile interpretation to identify the depth to gas front across the fjord. By combining these analyses, we find that the gas below most pockmarks in Loch Linnhe is between 1.4 m and 20 m deep. We anticipate that this work will help to understand the fate and mobility of sedimentary carbon in fjordic (marine) settings and advise offshore industry on the potential hazards posed by pockmarked seafloor regions even in nearshore settings.

Keywords: pockmarks; ArcGIS; hydroacoustic; hot-spot; marine; geo-hazard

1. Introduction

Gas within marine sediments was first recognised in seismic records 60 years ago and referred to as the 'becken effekt' or basin effect [1]. This acoustic phenomenon, commonly referred to as acoustic turbidity or gas blanking, is characterised by chaotic reflections with no apparent structure masking the stratigraphy below. This blanking effect is caused by gas bubbles affecting the acoustic and mechanical properties of the sediment, which in turn increases the amount of sound attenuation measured. Sediment cores taken from within an area of acoustic turbidity in the Irish Sea Basin confirmed this hypothesis [2]. The concentration of methane was high within this Irish Sea zone of acoustic turbidity with concentrations ranging from >100 nmol^{-1} to <10 nmol^{-1} within the uppermost 1.6 m of seabed sediment. Acoustic structures below this zone of turbidity are no longer visible, with internal reflections below these gas-charged horizons entirely or partially obscured. Zones of acoustic turbidity on hydroacoustic records can take different shapes and sizes. Descriptive terms such as acoustic curtains, blankets and plumes have been used to help differentiate between acoustically turbid zones with different lateral and vertical distributions [3]. These three forms have been used previously to show how acoustic signatures of gas-charged sediments can be related to underlying geological controls, based on acoustic datasets collected from UK nearshore regions (mainly boomer and pinger records) [3,4]. These workers identified zones of acoustic turbidity, in the form of curtains and blankets plus two other acoustic facies—white and black fringes—and showed that the strength and phase of the acoustic signal relates to different depositional environments. It has been suggested that certain terms (e.g., acoustic curtain and blanking)

are not necessary [5] and that only two types of gas-related acoustic turbidity can be reliably identified.

Further acoustic evidence of sub-seabed gas includes gas chimneys and plumes. Gas plumes are narrow zones of acoustic turbidity with distinct lateral boundaries, typically <50 m wide, and with an apparent connection to a gas source, which is likely biogenic [3–5]. Gas plumes have been observed as having numerous high-amplitude parabolic reflectors and can also appear as an amorphous cloud. Gas chimneys are narrow vertical zones of disturbance caused by gas migration. Some workers support the use of terms that describe the vertical migration of gas such as plume and chimney, as these indicate direct evidence of gas migration. Much work has been conducted to detect and map the 3D structures of gas chimneys in order to understand their role in hydrocarbon migration, as they can create unfavourable conditions for seabed infrastructure and lead to pockmark formation [6].

Identifying pockmarks and shallow sub-seabed gas is an essential part of determining the potential hazards posed to offshore infrastructure [7,8]. However, the degree to which pockmarks are considered a geohazard is still debated [9]. This is largely due to the formation of pockmarks being dependent on gas pressure, which can vary greatly. As such, a detailed understanding of pockmark formation and seabed fluid flow in certain offshore settings is still lacking. Pockmarks that have experienced long-term venting have been observed in the North Sea, where methane-derived authigenic carbonates (MDAC) have formed and been exposed on the seabed [10,11]. MDAC is considered an important geological structure worthy of marine protection status, typically within special areas of conservation (SAC). There is general agreement that pockmarks are indicators of hazardous seabed settings including tectonic/seismic activity [12,13], areas of potential gas hydrate and also potential seabed slumps and slides [13]. Pockmarks can also indicate the presence of deep hydrocarbon accumulations in offshore basins [14]. However, little work to date has explored the importance of pockmarks as geohazards in nearshore settings.

Seabed pockmarks are relatively widespread across the continental shelf around Scotland, occurring mainly in the North Sea sector, discovered during oil and gas surveys [11,15,16]. More recently, pockmarks have also been discovered further inshore within the fjords and fjord approaches of western Scotland [17,18], similar in size and bathymetric setting to those identified in the western fjords of Arctic Svalbard [19–21]. These fjordic environments are shown to be effective stores of organic carbon [22,23]. However, the presence of pockmarks indicate that these stores are not permanent and that gases, such as methane, can seep into the water column back into the marine carbon cycle [5,24]. Certain studies have shown that this gas can also enter the atmosphere [24,25], although this is dependent on water depth and local hydrographic/meteorological factors [26]. It is thought that pockmarks in Scotland's fjords are formed by the release of shallow biogenic gas, whereas those further offshore in the North Sea sector are related to deeper-seated thermogenic gas accumulations [15]. This is supported by research into the carbon signature of fjordic and offshore/shelf sediments, where the majority of organic carbon is stored within fjordic systems; however, localised hot-spots of organic and inorganic carbon can also be found in sediments of the wider continental shelf [27]. Regional mapping of pockmarks in Scottish west-coast waters has suggested a link between pockmark morphology, hydrographic setting and the activity history of pockmarks [18]. The authors have already mapped pockmarks within Loch Linnhe, part of a wider mapping initiative, and inferred the presence of widespread seabed gas/fluid escape (of unknown age). Previous unpublished research investigating the glacial history of the wider region also found some geophysical evidence of sub-seabed gas in the same inlet (or sea loch) [28,29]. However, neither of these studies fully explored the relationship between sub-seabed gas and the presence of pockmarks at the seabed. In this paper, we explore the three-dimensional spatial relationships between sub-seabed gas presence and pockmark formation in Loch Linnhe, to answer the following questions:

1. How widespread and how deep is the (near-surface) sub-seabed gas stored in Scotland's fjordic sediments?

2. What can the distribution of sub-seabed gas tell us about pockmark formation and possible trigger mechanisms?
3. Can we infer pockmark age relationships or activity status based on present-day gas presence or absence?

2. Materials and Methods

2.1. Study Site and Geological Setting

Loch Linnhe, on the west coast of Scotland, is a large fjord or sea loch, trending SW–NE, separated into two main basins. This study focuses on the outer basin and extends from the Corran Narrows in the north to the northerly tip of Lismore Island where the sea loch opens into the less-sheltered waters of the Firth of Lorn (Figure 1a). There are no prominent sills within the outer basin, so water flow is unrestricted. Hydrography of the region is estuarine whereby freshwater flows seaward and is replaced by saline water flowing at depth northward. Loch Linnhe is situated astride the south-westerly extension of the Great Glen Fault [30], which divides the bedrock of the region into the Moine metamorphic series and the Dalradian metamorphic series, composing the west and east shores of Loch Linnhe, respectively [31,32]. The last glacial activity in the Loch Linnhe catchment was during the Younger Dryas when outlet glaciers draining from Rannoch Moor via Glen Coe and Loch Leven coalesced with other smaller glaciers in Loch Linnhe forming a substantial tidewater glacier in the outer basin (Figure 1b). Numerical modelling experiments place the limit of the Younger Dryas glacier around Shuna Island [33]; empirical reconstructions are generally in agreement, although the precise timing of this late glacial ice-cap re-advance is still contested. Deglaciation of Loch Linnhe had probably occurred by 11.0 ka BP [28].
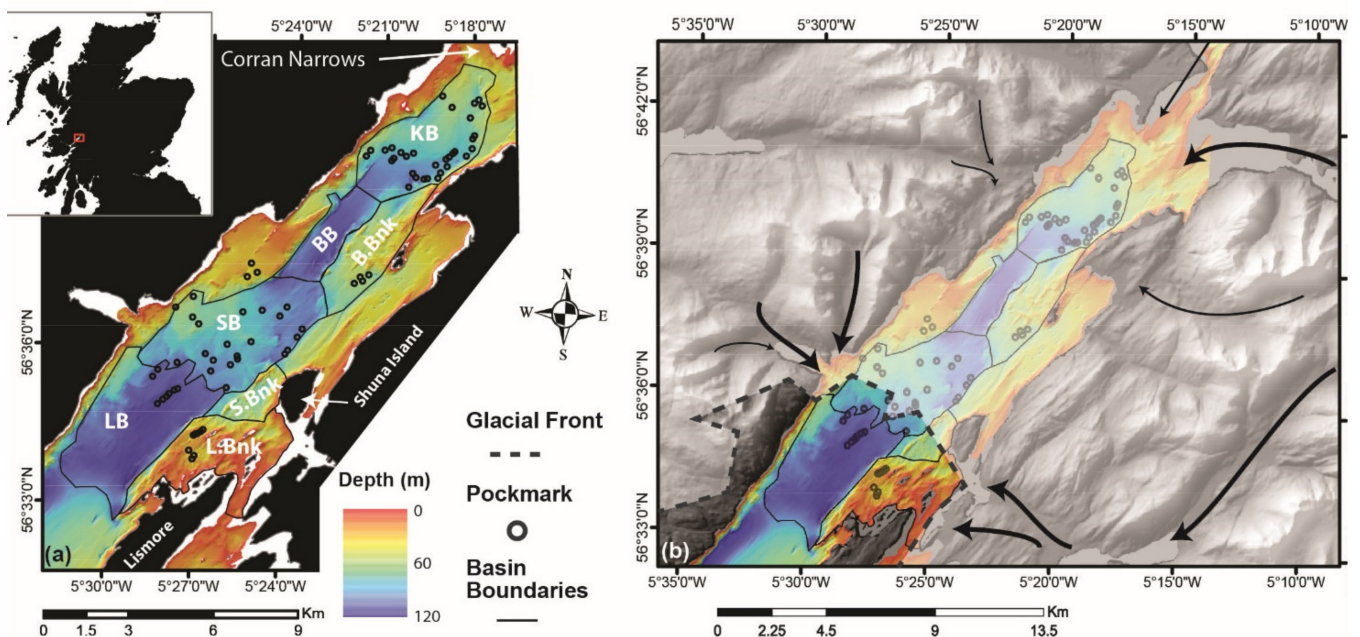
Figure 1. Maps of Loch Linnhe; (**a**) bathymetry of Loch Linnhe, location of pockmarks and basins; KB—Kentallen Basin, BB—Balnagowan Basin, B.Bnk—Balnagowan Bank, SB—Shuna Basin, S.Bnk—Shuna Bank, LB—Lismore Basin, L.Bnk—Lismore Bank; (**b**) map of the glacial ice cover during the Younger Dryas based on the model by [33]. Arrows show the main glacial flow from Rannoch Moor (west) and tributary glaciers from the east.

2.1.1. Multibeam Echo-Sounder Bathymetry

Loch Linnhe multibeam echo-sounder bathymetry (MBES) data were collected between December 2011 and July 2012 under Hydrographic Instruction 1371 as part of the Civil Hydrography Program (CHP). The data were processed to International Hydrographic Organisation (UKHO) order 1a specification [34]. The resultant raster was gridded

at 12 m resolution and processed in ESRI ArcGIS. The MBES dataset is made available through the UKHO bathymetry portal where further information can be found on the survey methodology, data collection and specification [34].

2.1.2. Sub-Seabed Geophysical Data

The original printed CODA seismic records were used for the analysis; these were obtained from the Scottish Association for Marine Science (SAMS). The seismic survey was conducted in 2010 using an Applied Acoustic AA300 surface-tow boomer. Vertical scale lines show the two-way travel time interval of 20 msec measuring 33 mm on paper records. Following a sound speed of 1500 msec for unconsolidated sediment and 2000 msec for consolidated sediment, this provides us with an approximate depth conversion of 1 mm = 0.45 m–0.60 m. Horizontal scale lines record the 'fixes', which were recorded at 1-minute time intervals. With an average constant ship speed of 4.5 knots, the approximate distance between fixes is 140 m; this is confirmed by ArcGIS analysis. Seismic profiles were scanned (digitised) and interpreted—building on the existing, unpublished seismo-stratigraphy [28].

An ESRI shapefile containing the position of seismic lines and fixes was obtained from the British Geological Survey (BGS) Offshore GeoIndex (https://www.bgs.ac.uk/map-viewers/geoindex-offshore (accessed on 29 January 2019)). Location data for each pockmark mapped within Loch Linnhe were taken from our existing published dataset [18]. The mapping process used the BGS seabed-mapping toolbox [35]. The toolbox uses several tools within ESRI ArcGIS to analyse the bathymetry, semi-automatically identify pockmarks and place a point (shapefile) at the deepest point within the delineated pockmark—representing the centre of the pockmark. A detailed description of the seabed mapping toolbox is presented elsewhere [35].

2.2. Inverse Distance Weighting

Within ArcGIS the inverse distance weighting (IDW) tool was used to interpolate the vertical distance to the gas front. IDW uses the principle that further points have less of an effect on nearby points and interpolates a surface based on this. The distance to the gas front was measured by recording observations of acoustic turbidity at each seismic fix—approximately 140 m apart. If no gas was observed, then an NA value was recorded and not processed during IDW interpolation.

2.3. Hot-Spot Analysis

Optimized hot-spot analysis within ArcGIS was used to identify hot-spots of pockmark formation. The tool uses the Getis-ord Gi* statistic, which implements the principle that nearby features are more related than distant features. Two main variables can be set by the user: cell size and neighbourhood distance. The default values are calculated by the tool using spatial auto-correlation, which identifies the distance band of peak clustering of the features. This is generally used as a guide to inform the user, but it is recommended that variables are set according to the specific question being tested.

For this analysis, variables were set to test the question whether pockmark hot-spots have formed. Previous studies suggest that when pockmarks form, they act as the primary drainage channels for all surrounding gas up to half the nearest neighbour distance, at which point gas theoretically vents from the 'new' nearest pockmark to reduce pressure. This distance of half the nearest neighbour distance is termed the 'exclusion zone' [36] within which theoretically no other pockmarks will form. Nearest neighbour distance was calculated using the average nearest neighbour tool within ArcGIS. If this assumption is violated, we consider this a hot-spot, and by inference, that the volume/pressure of gas within the region is unable to escape effectively through a single pockmark. In these situations, theory would suggest that one pockmark is not able to sufficiently reduce the gas pressure within the area. Using this 'exclusion zone' concept, the cell size for hot-spot analysis was set at half the average distance to the nearest neighbour, and the

neighbourhood distance was set as the average distance to the nearest neighbour. Thus, if more than one pockmark occurs within the exclusion zone, then a hot-spot is immediately recognised; if further pockmarks are observed within the neighbourhood distance then these areas are also considered hot-spots at varying degrees of confidence.

3. Results

3.1. Hot-Spot Analysis

Hot-spot analysis was conducted over three scales (Figure 2) to identify regions where statistically more pockmarks have formed in the study region and highlight regions that require further investigation. The first targeted all pockmarks within the outer basin of Loch Linnhe. The analysis calculated an average nearest-neighbour distance of 220.4 m, which was used as the analysis neighbourhood with half this distance (110.2 m) used as the cell size. The analysis identifies that the majority of pockmarks are forming in localised hot-spots within basins, with the exception of SB (Figure 2a). The second scale of analysis targeted only the pockmarks that are within the region covered by the seismic survey. A nearest-neighbour distance of 285 m was used as the analysis neighbourhood and 142.5 m for the cell size. This hot-spot analysis produced similar results to the first scale of analysis (Figure 2b). The third analysis only targeted pockmarks in the region where gas was observed on seismic records. In this case, a nearest neighbour distance of 402 m was used as the analysis neighbourhood and 201 m for the cell size. The third analysis shows hot-spots within LB, KB and B. Bnk (Figure 2c). No hot-spots were identified at any scale within BB, and the majority of pockmarks within SB do not form hot-spots at any scale.
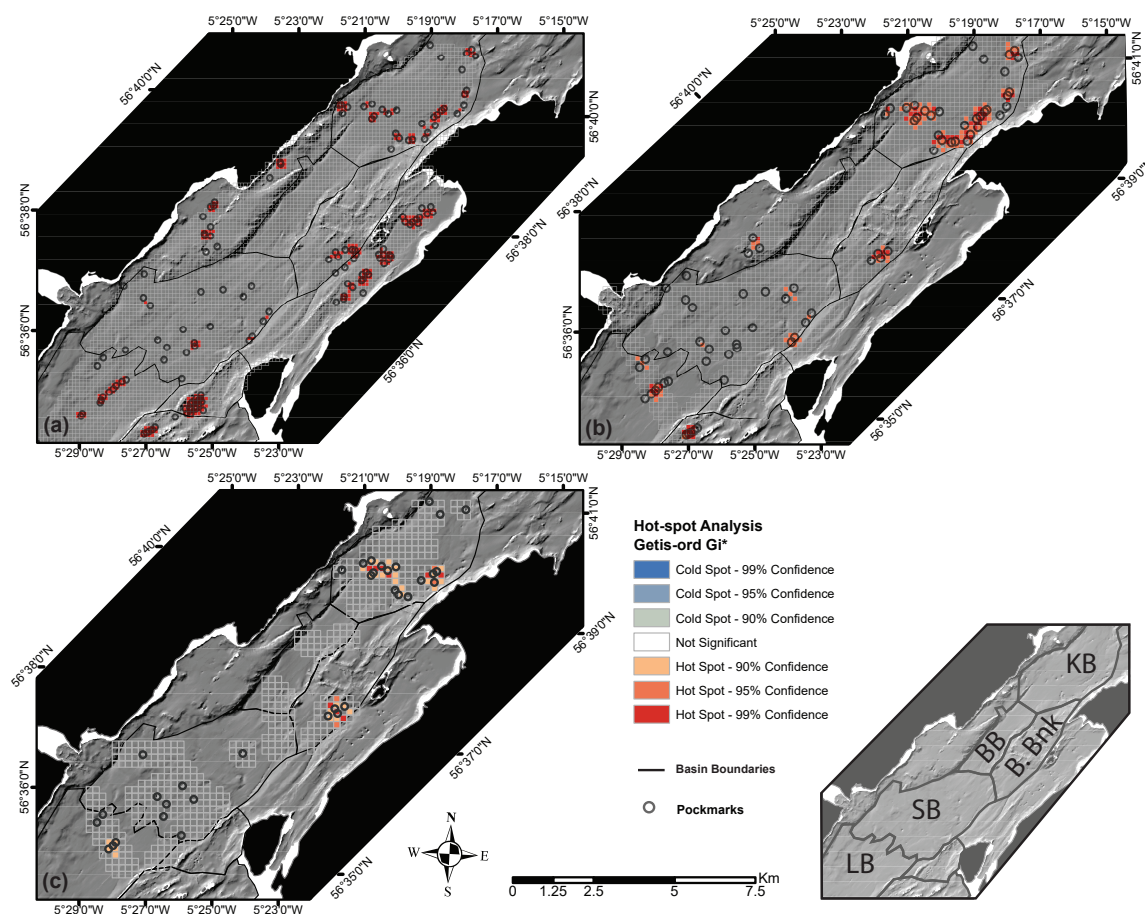
Figure 2. Hot-spot analysis using the Getis-ord Gi* statistic of pockmarks within Loch Linnhe along with an inset map showing main basins mentioned in Figure 1; (**a**) hot-spot analysis of all pockmarks within Loch Linnhe; (**b**) hot-spot analysis of pockmarks that occur within the region of the boomer seismic survey; (**c**) hot-spot analysis of pockmarks where gas was observed in seismic profiles.

3.2. Seismic Interpretation

Our seismic interpretation has been adapted from the Loch Linnhe seismic facies (LLSF) framework outlined by McIntyre (Table 1) [28]. A common feature in every line is the L1 reflector. This reflector occurs at the base of LLSF5.

Table 1. Seismic facies of Loch Linnhe and their interpretations adapted from McIntyre [28].

Seismic Facies	Seismic Characteristic	Interpretation	Setting
LLSF5	Strong, continuous, parallel reflectors draped over topography.	Youngest unit, 3–4 m thick. Thin or absent on steep slopes. Terrigenous-derived, organic/inorganic, deposited under suspension.	(Holocene) Marine
LLSF4	Continuous, parallel, sheeted reflectors, draped in deep basins.	Directly under LLSF5 (L1) reflector. Up to 45 m deep. Thin or absent on bathymetric highs.	(Younger Dryas) Glaciomarine (distal)
LLSF3	Strong, continuous to discontinuous. Parallel to sub-parallel.	Occurs below LLSF4, >80 m deep. Absent from banks and shallows.	(Younger Dryas) Glaciomarine (proximal)
LLSF2	Lacking internal structure, chaotic reflections. Sometimes blanks underlying seismic structures.	(a) Present at the base of many slopes, occupying regions that would otherwise contain LLSF3/4. Usually does not, or only partially, obscures underlying facies. (b) Occurs as wide regions with abrupt to diffusive initial reflection. Abrupt vertical boundaries where it obscures LLSF3/LLSF4. Usually completely obscures any other reflectors. May also form as isolated domes. Interpreted as acoustic blanking due to gas scattering or attenuated seismic signal.	(a) Slumps. (b) Gas.
LLSF1	Strongly hyperbolic to chaotic. Discontinuous reflectors.	Present as the basal unit in most regions. In other regions they can occur as discontinuous reflections within LLSF2. Interpreted as ice-contact deposited proglacially as moraines or sub-glacially. Compacted, unsorted clay—boulder in size. Possibly bedrock (acoustic basement).	(Younger Dryas) Diamict or bedrock

The clearest representation of gas within the study region is in the form of acoustic turbidity (blanking) as seen within numerous seismic line profiles (Figure 3). This is identified as LLSF2b (Table 1) and can be observed at the southerly and northerly regions of Loch Linnhe. Acoustic turbidity can be observed in the form of undulating curtains (Figure 3 Line A), or associated with reflector pull-downs interpreted as a chimney structure (Figure 3 Line B), or as widespread blanket (Figure 3 Line C). Regions of acoustic turbidity are often found to be near pockmarks, where gas has vented into the water column during pockmark formation/activity.

Pockmark 2 shown in Figure 4 Line A was identified and described as a 'deep' pockmark [18]; that is a statistically deeper-than-average pockmark depth (based on depth/area ratio) across the studied sites around western Scotland. The L1 reflector is not present within the centre of this pockmark. No clear signs of gas, LLSF2b, are observed beneath pockmarks 1 and 2 (Figure 4 Line A:B). The seismic facies are chaotic and obscure in places; however, they do not have the same acoustic turbidity characteristics commonly attributed

to gas. Seismic lines B and C show the classic example of acoustic turbidity (LLSF2b), interpreted as gas. Line B shows a variable depth to the gas front and contains a pockmark. Line C shows widespread coverage of LLSF2b, here termed a 'gas blanket'.
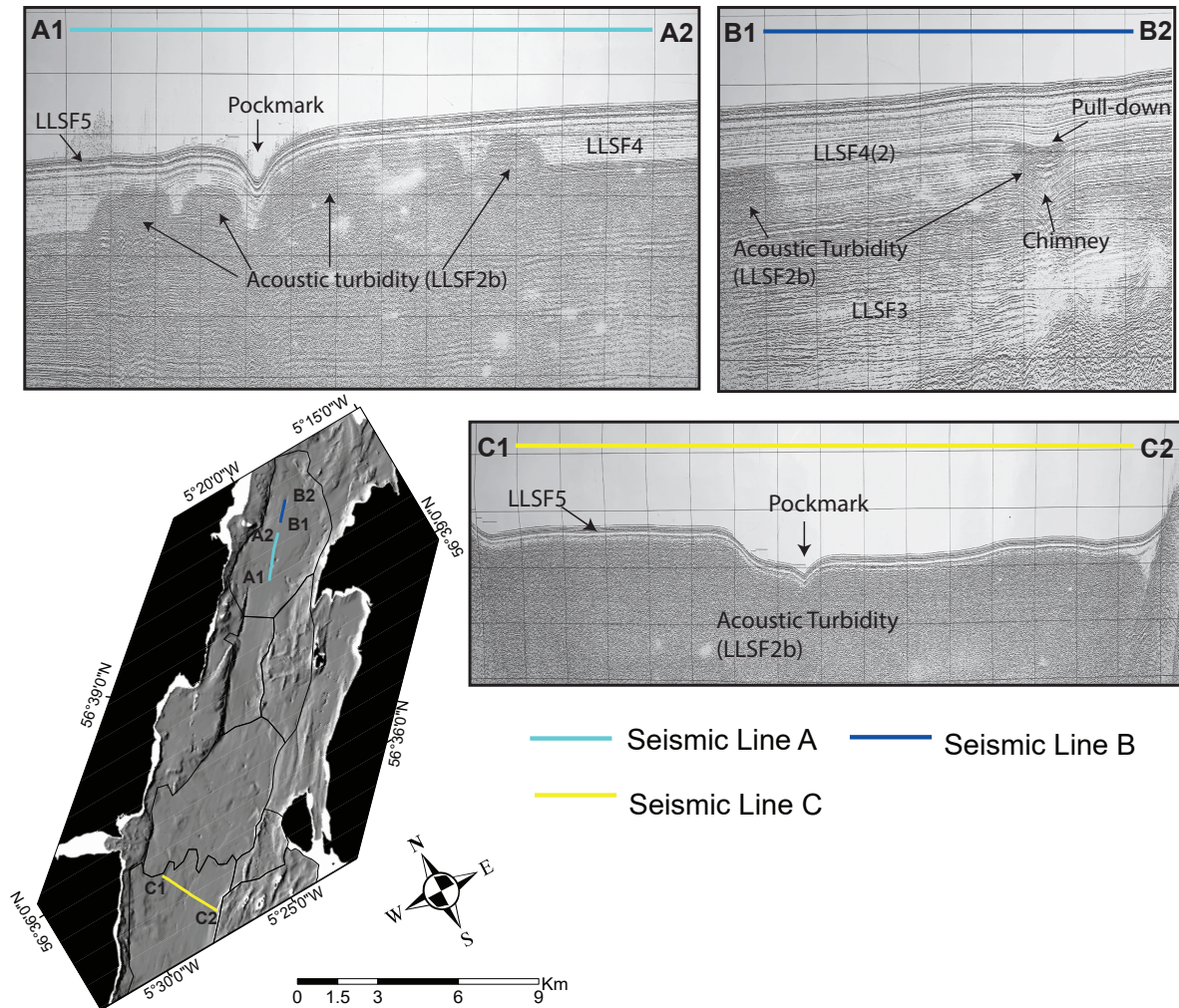

Figure 3. Selected Loch Linnhe seismic lines containing evidence of sub-seabed gas/fluid accumulation in the form of acoustic turbidity (or blanking), seismic chimneys and pull-down reflectors. Map shows the position of seismic lines and corresponding profiles (colour coded).

The seismic line that extends through BB from KB in the north to SB to the south contains several examples of pull-down reflectors (Figure 5). The most northern section of Line B (Figure 5) shows the clearest evidence of LLSF2b, interpreted as gas at this site. This acoustic turbidity continues at greater depth until it forms the front to a section of LLSF2. This front is very stable but is not parallel to the seabed. It appears to occupy the region that would otherwise be filled with the older LLSF4 (1) unit. We are unable to definitely interpret this facies as gas due to the incomplete blanking of deeper reflectors. Sections of pull-down reflectors are recorded within LLSF3. It is likely that this area of LLSF2 is slump material or sediment that has lost all internal structure due to it becoming 'quick', with occasional pockets of gas. A similar interpretation is made for LLSF2 in Line B. No evidence of LLSF2 is observed in Line C. We interpret this section as not containing gas. A section of acoustically stronger reflectors lies between the boundary of LLSF4 (2) and LLSF4 (1). This is interpreted as a unique lens of higher density material—possibly a short-lived

debris flow event. Further clear evidence of pull-down reflectors is present within Line C, extending throughout the depth of LLSF3 and towards the boundary with LLSF1.
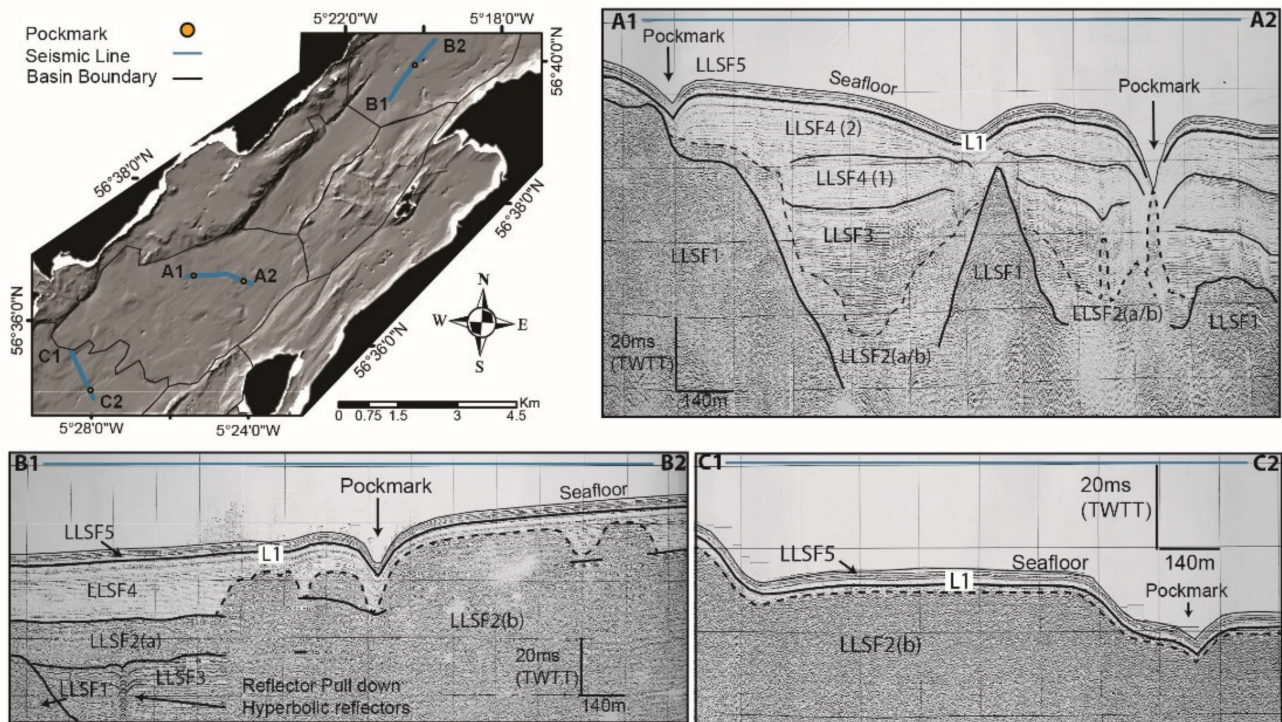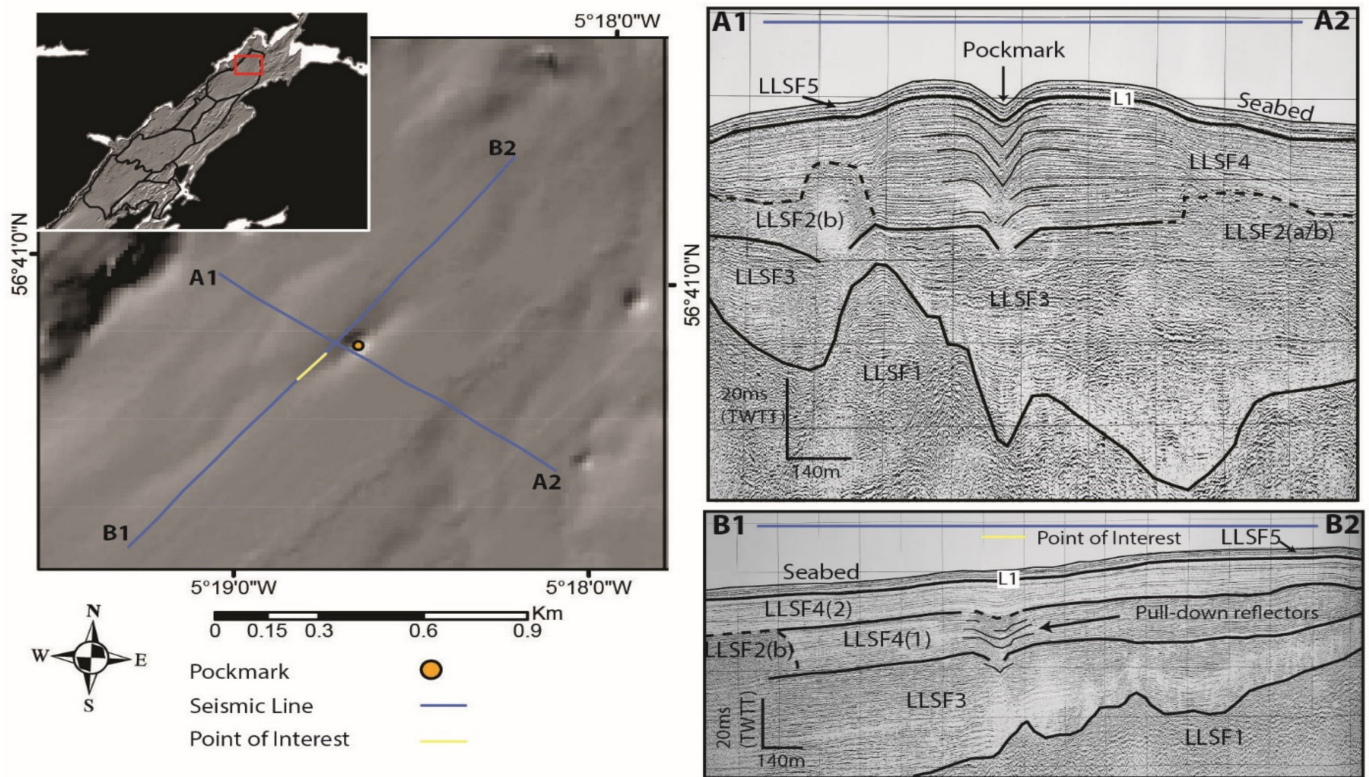

Figure 4. Seismic analysis of selected lines across pockmarks. Map shows the position of seismic lines, basin boundaries and the location of pockmarks that appear on the seismic line. Labelled seismic line sections correspond to the seismic profiles A:C. Profiles B and C are also shown in Figure 4 where gas-associated features are indicated.
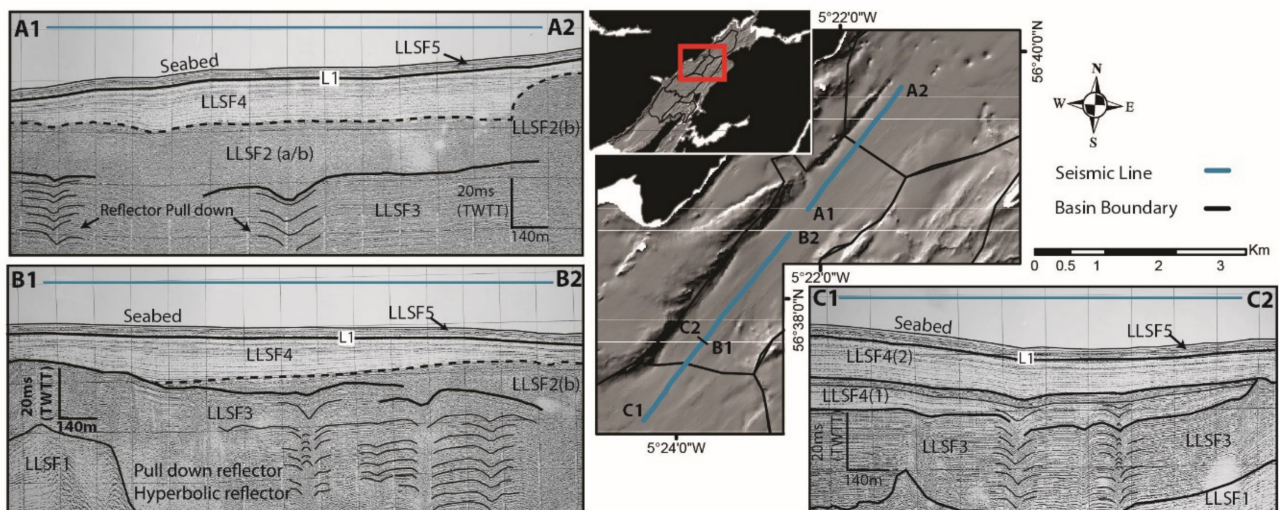
Figure 5. Analysis of selected seismic lines that contain pull-down reflectors. Map shows the position of seismic lines, basin boundaries. Labelled seismic lines sections correspond to the seismic profiles A:C. Dotted lines within seismic profiles show the position of the surface reflector for LLSF2, where LLSF2b indicates acoustic turbidity.

Further examples of pull-down reflectors are closely related to the presence of pockmark 6 within KB (Figure 6 Line A). The pull-down reflectors are directly below pockmark 6 and extend into the underlying LLSF3. Evidence of gas is seen on either side of the pockmark in this profile but not directly below the pockmark. Further evidence of gas is recorded at the start of Profile H. Pull-down reflectors are also recorded immediately

southwest of pockmark 6. The internal reflections at this point of interest are discontinuous and partially obscured, indicating that sediment containing gas may be present here.

Figure 6. Analysis of selected seismic lines containing pockmarks and pull-down reflectors. Map shows the position of seismic lines, basin boundaries and the location of pockmarks that appear on seismic line. Labelled seismic lines sections correspond to the seismic profiles A:B. Seismic Line B is also shown in Figure 4 where gas-associated features are indicated.

3.3. IDW

The interpolated raster shows locations where sub-seabed gas was identified from seismic data. The gas shows a depth range of 3.7–50 msec two-way travel time (TWTT) (Figure 7a). Gas was observed within all regions of the outer basin. The regions of most widespread gas occur in LB and KB (see Figure 1 for locations); in all other regions, gas forms isolated zones. Generally, gas was seen in close proximity to pockmarks. Figure 7b shows the number of pockmarks that lie directly above a region of gas-rich sediment. Thirty-five pockmarks have gas directly beneath their centres. Of these, 29 pockmarks occur above a gas front 3.7–20 msec deep, five pockmarks above a gas front at 20–30 msec depth, and one pockmark is located above possible gas at 40–50 msec depth; this pockmark is further investigated in the discussion. Thirty-two pockmarks occur in regions where gas could not be observed; however, this result largely reflects the incomplete seismic survey coverage in Loch Linnhe, making it not possible to observe the presence/absence of gas between geophysical lines.
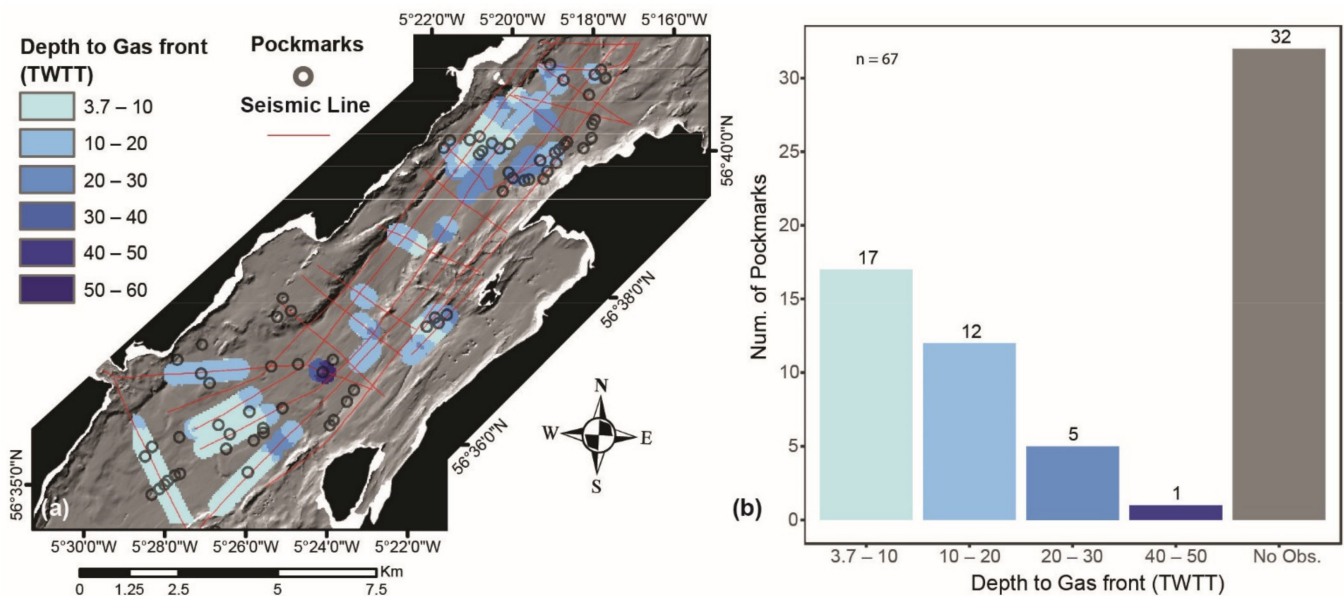
Figure 7. Study area showing boomer seismic survey lines and pockmarks; (**a**) depth to gas front (TWTT), where gas was observed in seismic profiles; (**b**) bar-plot showing number of pockmarks within each depth to gas front band.

4. Interpretation and Discussion

Quantitative hot-spot analysis has been used to investigate whether pockmark hot-spots in Scottish fjords, such as Loch Linnhe, relate to the distribution of sub-seabed gas seen in hydroacoustic (boomer seismic) data. We based this analysis on the principle of an exclusion zone [36]. Depending on the number of pockmarks used in the analysis, the average nearest-neighbour distance changes. We conducted this analysis on three spatial scales where the area of interest, and therefore, the number of pockmarks present, decreases in size.

We found that hot-spots were consistently identified at all scales of analysis within the KB, LB and SB sub-basins (Figure 2). In these three regions, we also found widespread evidence of sub-seabed gas, with a gas front between 3.7–20 msec deep (TWTT). We conclude that by applying the exclusion zone principle [36], we have developed a suitable model for identifying regional gas-rich sediment through pockmark hot-spot identification. We note that pockmark hot-spots are absent from much of LB and BB. This is likely due to the thinner accumulations of glaciomarine sediments containing less organic material necessary for the formation of pockmarks. The thinning of LLSF4 observed within these regions [28] is interpreted as areas of non-deposition resulting from increased bottom currents typical in narrower bathymetric settings.

Interpolating a grid (raster) based on the presence of gas within seismic records is a useful method for not only mapping the distribution of gas within a region but also for identifying its depth range. We map sub-seabed gas throughout the study site: either widespread in KB, northwest LB and S.Bnk, or as isolated pockets, such as in BB (Figure 7). The depth range to the gas front recorded beneath most pockmark centres is between 3.7–20 msec TWTT (Figure 7b). Our seismic analysis supports the conclusion that gas-rich sediments, observed in seismic records as LLSF2b, stratigraphically relate to LLSF4 in age, based on the depths of the gas fronts [28] and surrounding facies. Facies LLSF4 is interpreted as distal glaciomarine sediment laid down during ice wastage at the end of the last (Late Weichselian) ice-sheet glaciation or during the Younger Dryas [28]. Despite being deposited within a fjordic glacial environment, these muddy sediments must contain enough organic matter to support microbial communities and produce gas. Deposition of organic matter in contemporary nearshore glacial settings has been found within the fjords of western Svalbard [37] where gas-charged sediment is observed resulting from organic matter associated with marine productivity distal to the glacial margin. Further

examples of biogenic gas accumulations within Late Pleistocene (Weichselian) glaciomarine muds are found in the North Sea Basin [38] and in one or two nearshore basins off northwest Scotland [39–41]. Within Loch Linnhe, total carbon content has been estimated at 92.28 Mt [23], but with very low C/N ratios recorded within the uppermost 4 m of sediment [28]. This is likely attributed to relatively high inorganic carbon content resulting in poor preservation of organic carbon [42,43]. Gas-charged sediments of biogenic origin have also been found within the glaciomarine Emerald Silt Formation on the Canadian Atlantic continental shelf [44]. In that setting, however, the authors argue that thermogenic sources of gas must be present, as they deem it unlikely that the sediment package contained enough organic matter to form a sufficient volume of gas for pockmark formation. Owing to the predominantly metamorphic Precambrian bedrock, a thermogenic source of gas is unlikely in Loch Linnhe. Contrary to the findings on the Canadian Atlantic shelf, distal glaciomarine sediments within fjordic environments off Svalbard can contain enough organic carbon to generate shallow sub-seabed gas accumulations [19].

Our study suggests that relatively distal glaciomarine material on the floor of Loch Linnhe contains enough organic material to promote the build-up of shallow biogenic gas (<50 msec deep). From these findings, we suggest that biogenic gas can form in nearshore sedimentary basins where sediments containing organic matter were deposited rapidly during the warming events at the end of the last (Weichselian) ice-sheet glaciation and/or at the Younger Dryas/Holocene transition. Rapid sediment accumulation in these time intervals has been reported in nearby Loch Etive [45] and in Loch Broom, NW Scotland, where there is similar geophysical evidence of shallow (biogenic) gas below the seabed [17]. Rapid sedimentation is also reported in numerous glaciated high-latitude fjords, such as Kongsfjorden, Svalbard with sedimentation rates as high as 10 cm a^{-1} [46,47] Svendsen 2002. This organic material would have preferentially accumulated in regions where hydrodynamic flow was restricted by bathymetric obstacles, such as moraines or bedrock highs, or in larger deeper-water basins with weak bottom currents [28]. We suggest that the complex interactions between hydrodynamics and seabed topography in Loch Linnhe resulted in the patchwork of gas pockets now present within SB and BB and the more widespread gas accumulations in KB and northwest LB—the latter perhaps representing local depocentres for organic material in areas of little or no bottom current.

The L1 reflector has been identified on seismic data throughout the study area and is thought to represent the onset of a full interglacial environment in Loch Linnhe [28]. Throughout LLSF4, the environment changes from distal glaciomarine to Holocene paraglacial conditions before its transition into full interglacial marine conditions (represented by LLSF5). LLSF5 represents Holocene sedimentation where vegetation has stabilised much of the surrounding terrestrial topography, resembling the present-day landscape. A similar reflector termed E1 was identified in the adjacent fjord of Loch Etive [48] where radiocarbon-dated shells yielded an age of 10,240 +/- 82 cal yr BP. Shells from the L1 reflector in Loch Linnhe provide radiocarbon dates of 10,313 +/- 100 and 8347 +/- 73 cal yr BP [28]. It is assumed that the transition from late glacial (cold) to interglacial (warm) marine conditions occurred at a broadly similar time across western Scotland ca. 10.5–11.5 cal ky BP.

Our results show that this Holocene sediment package (LLSF5) is of approximately uniform thickness across the study area, even within the majority of pockmarks. We interpret this to reflect generally constant, spatially uniform sedimentation rates across the sea loch during the Holocene. Since this unit, including the L1 reflector, is present within the majority of pockmarks in the study area, it is likely that the majority of pockmarks formed prior to 10.3 cal ky BP and have, at most, only been periodically venting low volumes of gas with insufficient fluid flow to remove or inhibit sedimentation. This is supported by the results on the morphology of pockmarks in the region [18], where 51% of pockmarks are classed as 'regular' due to their shallow profile and low depth: area ratio. This class of pockmarks is common in the waters around western Scotland. 'Regular' pockmarks are interpreted as being less active then 'deep' pockmarks [18]. The only pockmark imaged in seismic records where the L1 reflector is not observed is pockmark

2 (Figure 4, Line A). Due to the absence of the L1 reflector and the thin cover of LLSF5, we interpret this as the most recently active pockmark within Loch Linnhe. However, the strongly V-shaped depth profile of the pockmark and presence of the L1 reflector in the flanks of the pockmark suggest that it started forming prior to ~10.3 ky BP but has been regularly active throughout the Holocene. This interpretation is supported by semi-automated classification of pockmarks in this region [18]. This unusual pockmark was classed as 'deep' by Audsley et al. [18] who interpreted it as one of a number of pockmarks with a longer activity time or more energetic gas/fluid venting. Interestingly, we find little seismic evidence of gas directly below this pockmark. We map LLSF2 below pockmark 2, as separate narrow vertical zones in the surrounding facies and connecting with the base of the pockmark. However, in this location, this facies does not have the typical acoustic character commonly associated with gas.

Pockmarks can also form through venting of fluids without gas present. Pockmarks forming from non-gas-related fluid discharge have been observed in MacBeth fiord, Baffin Island [49] and Isfjorden, Svalbard [50]. This phenomenon has been described to occur either in ice-proximal settings, where buried ice can be present regions of very rapid sediment accumulation or where groundwater is driven under glaciomarine sediments by the hydrostatic pressure of surrounding topography [49]. From this evidence, we conclude that this deep pockmark formed prior to 10.1 ky BP and has been regularly active throughout the Holocene, although the genesis of this pockmark may be related to another form of fluid discharge and not the expulsion of biogenic gas.

We also observed V-shaped pull-down reflectors on seismic records across much of the study area, closely related to sub-seabed gas accumulations and/or pockmarks (Figures 4–6). These V-shaped reflectors are generally found in LLSF3 and terminate near the lower boundary of LLSF4 but can also be found directly below pockmarks. Where pull-down reflectors are seen within LLSF3, they were previously interpreted [28] as examples of faults associated with isostatic rebound or examples of relict fluid-escape pockmarks below the present-day seabed, as seen elsewhere [49]. Where pull-down reflectors are recorded directly below pockmarks in Loch Linnhe, we interpret these as acoustic artefacts resulting from the attenuation of sound waves due to gas or as the morphology of the former seabed. In the case of pockmark 6 (Figure 6, Line A), we find that the reflectors change from steep sided V-shaped to more rounded u-shaped reflectors close to seabed. We conclude that this particular pockmark is probably inactive and that pull-down reflectors represent the palaeo-seabed at depth.

Throughout the study area, we observe several examples of gas migration. According to [3], these can be either acoustic blankets, curtains (100–500 m wide) or plumes (<50 m wide). It has been suggested [5] that terms other than acoustic blanket and plume are unnecessary and do not add to the interpretation of gas migration within marine sediments. We argue that additional descriptive terms are useful, as they form a possible continuum of stages potentially showing the progression of gas migration. Where we observe gas blankets (Figure 3, Line C), the gas front is uniform and near seabed, even when a pockmark is present; this is thought to represent a region where gas pressure is controlled by the diffusion of gas into the Sulphate Methane Transition Zone (SMTZ), where it is consumed by microbial communities [51]. Within this zone, methane is consumed, which effectively lowers the pressure of the gas-rich fluids stored below. This finding is supported by the diffusive boundary at the gas front below 3.7 msec (Figure 3, Line C). At this site, the pockmark is no longer the primary gas-venting site, and the presence of LLSF5 overlying the pockmark indicates that it is no longer active. This pockmark probably formed prior to the widespread migration of gas and provided the only vent in the region to lower the pressure of shallow gas. We interpret the present-day distribution of gas blankets at this site to have been caused by the vertical migration of gas and the formation of in situ gas from microbial communities within younger sediments containing organic matter.

We also observe gas curtains in Loch Linnhe (Figure 4, Line B). These curtains (100–500 m wide) are seen at the flanks of pockmarks and can be related to deeper gas

blankets (Figure 4, Line B). Between these gas curtains are regions where the acoustic signal is not interrupted by gas, these regions are termed 'acoustic windows' and provide an insight into the sediment facies otherwise obscured by gas blanking. From our analysis, we infer that gas is strongly associated with LLSF4, consistent with the depth of the gas front (Figure 7b) and the relative thicknesses of acoustic facies (Table 1). It has been shown that gas concentrations in sediment within curtains and blankets are significantly higher than within acoustic windows [2], explaining the acoustic turbidity or blanking effect seen in geophysical profiles. We also infer that curtains form above the deepest parts of basins where sediment thickness is greatest [3,4]. We propose that curtains and plumes can form by gas migrating within the flanks of pockmarks. Here, internal weaknesses in the sediment resulting from previous (now inactive) pockmark formation reach close to the seabed allowing the gas to be consumed within the SMTZ. Over time, gas migration and continued in situ gas formation, within shallow sediments containing organic carbon, spread laterally forming a gas blanket. An alternative hypothesis for the formation of gas curtains and plumes is that when they are halfway between the seabed and its source, the chance of an intermittent pockmark formation is high [52]. They may also, in the absence of structural weaknesses, be associated with further pockmark formation [52]. The migration of gas and further gas formation by microbial activity can lead to sufficient pressures to form a pockmark at seabed. It is possible that pockmarks located where gas is observed within the near-surface sediment are still periodically active [18]. In these settings, gases such as methane are released into the water column to re-join the marine carbon cycle. The age and activity status of pockmarks in west coast Scottish waters is still unknown, but due to the depth of many pockmarks in Loch Linnhe, it is likely that they have experienced a long activity history [18]. Due to these uncertainties, we cannot calculate the volumes of 'stored' carbon released into the marine column in Scottish waters. This should be a key question for future research.

We show that the distribution of sub-seabed gas and pockmarks in Loch Linnhe are associated and generally co-occur within localized hot-spots or pockets. The presence of shallow gas accumulations and pockmarks in Loch Linnhe suggest that these specific regions represent depocentres of organic carbon since deglaciation. Within these regions, we would expect higher contents of sedimentary carbon compared to the lower contents reported elsewhere in the loch [28]. However, the formation of pockmarks within Loch Linnhe may not be due to gas pressure alone. Due to the unknown quantities of buried organic carbon and the shallow nature of the sub-seabed gas, we must consider other trigger mechanisms for pockmark formation. Seismic activity and the reactivation of faults might also be a trigger. Western Scotland is a region where numerous earthquakes have been recorded since 1597 [53]. The presence of the Great Glen fault running through Loch Linnhe makes a seismic trigger for gas release very possible in this region.

Finally, we suggest that the identification of pockmarks and shallow sub-seabed gas within a nearshore region should not always be considered as a hazard, particularly when gas is at shallow depth (<100 m deep). It is likely that shallow (3.7–20 msec) gas curtains/blankets contain relatively small volumes of low-pressure gas that can be consumed by microbial activity in the SMT—seen as a diffusive upper boundary in boomer profiles. We concur that, in these situations, pockmark formation releases pressure within marine sediments and may increase overall substrate stability [9]. Additionally, we suggest that pockmarks in this Scottish fjord probably formed within local depocenters of sediment containing higher proportions of organic carbon compared to surrounding regions, where much of the sediment can be gas free. However, we suggest that gas plumes, which are typically deeper, may pose a potential hazard if pathways of egress are available, as this gas will have had little opportunity to reduce in pressure. Therefore, to inform industry on potential geohazards in fjordic environments, both bathymetric and sub-bottom geophysical surveys are required to identify (i) fluid-release pockmark hot-spots, (ii) thick muds potentially containing high-quantities of organic carbon and (iii) the depth of shallow

sub-seabed gas. Assessing these factors could be used to gauge whether gas pressures and volumes in quaternary sediments would be hazardous to seabed infrastructure.

References

1. Schuller, V.F. Untersuchungen uber die machtigkeit von schlickschichten mit hilfe des echographen. *Dtsch. Hydrogr. Zeitsehrift* **1952**, *5*, 220–231. [CrossRef]
2. Jones, G.B.; Floodgate, G.D.; Bennell, J.D. Chemical and microbiological aspects of acoustically turbid sediments: Preliminary investigations. *Mar. Geotechnol.* **1986**, *6*, 315–332. [CrossRef]
3. Taylor, D.I. Nearshore shallow gas around the U. K. coast. *Cont. Shelf Res.* **1992**, *12*, 1135–1144. [CrossRef]
4. Baltzer, A.; Tessier, B.; Nouzé, H.; Bates, R.; Moore, C.; Menier, D. Seistec seismic profiles: A tool to differentiate gas signatures. *Mar. Geophys. Res.* **2005**, *26*, 235–245. [CrossRef]
5. Judd, A.; Hovland, M. *Seabed Fluid Flow: The Impact on Geology, Biology and the Marine Environment*; Cambridge University Press: Cambridge, UK, 2007.
6. Meldahl, P.; Heggland, R.; Bril, B.; de Groot, P. The chimney cube, an example of semi-automated detection of seismic objects by directive attributes and neural networks: Part I methodology. In *SEG Technical Program Expanded Abstracts 1999*; Society of Exploration Geophysicists: Tulsa, OK, USA, 1999.
7. Camargo, J.M.R.; Silva, M.V.B.; Júnior, A.V.F.; Araújo, T.C.M. Marine geohazards: A bibliometric-based review. *Geosciences* **2019**, *9*, 100. [CrossRef]
8. Orange, D.L.; García-García, A.; McConnell, D.; Lorenson, T.; Fortier, G.; Trincardi, F.; Can, E. High-resolution surveys for geohazards and shallow gas: NW Adriatic (Italy) and Iskenderun Bay (Turkey). *Mar. Geophys. Res.* **2005**, *26*, 247–266. [CrossRef]
9. Riboulot, V.; Imbert, P.; Cattaneo, A.; Voisset, M. Fluid escape features as relevant players in the enhancement of seafloor stability? *Terra Nov.* **2019**, *31*, 540–548. [CrossRef]
10. Gafeira, J.; Long, D. Geological investigation of pockmarks in the Braemar Pockmarks and surrounding area. *JNCC* **2015**, *571*, 1–92.
11. Böttner, C.; Berndt, C.; Reinardy, B.T.I.; Geersen, J.; Karstens, J.; Bull, J.M.; Callow, B.J.; Lichtschlag, A.; Schmidt, M.; Elger, J.; et al. Pockmarks in the Witch Ground Basin, Central North Sea. *Geochem. Geophys. Geosystems* **2019**, *20*, 1698–1719. [CrossRef]
12. Hasiotis, T.; Papatheodorou, G.; Kastanos, N.; Ferentions, G. A pockmark field in the Patras Gulf (Greece) and its activation during the 14/7/93 seismic event. *Mar. Geol.* **1995**, *130*, 333–344. [CrossRef]
13. Hovland, M.; Gardner, J.V.; Judd, A.G. The significance of pockmarks to understanding fluid flow processes and geohazards. *Geofluids* **2002**, *2*, 127–136. [CrossRef]
14. Fannin, N.G.T. *Use of Regional Geological Surveys in the North Sea and Adjacent Areas in the Recognition of Offshore Hazards*; Institute of Geological Sciences, Continental Shelf Division: Berlin, Germany, 1979.
15. Hovland, M.; Sommerville, J. Characteristics of two natural gas seepages in the North Sea. *Mar. Pet. Geol.* **1985**, *2*, 319–326. [CrossRef]
16. Hovland, M.; Judd, A.G.; King, L.H. Characteristic features of pockmarks on the North Sea Floor and Scotian Shelf. *Sedimentology* **1984**, *31*, 471–480. [CrossRef]
17. Stoker, M.; Bradwell, T.; Wilson, C.; Harper, C.; Smith, D.; Brett, C. Pristine fjord landsystem revealed on the sea bed in the Summer Isles region, NW Scotland. *Scottish J. Geol.* **2006**, *42*, 89–99. [CrossRef]
18. Audsley, A.; Bradwell, T.; Howe, J.A.; Baxter, J.M. Distribution and classification of pockmarks on the seabed around western Scotland. *J. Maps* **2019**, *15*, 807–817. [CrossRef]
19. Howe, J.A.; Moreton, S.G.; Morri, C.; Morris, P. Multibeam bathymetry and the depositional environments of Kongsfjorden and Krossfjorden, western Spitsbergen, Svalbard. *Polar Res.* **2003**, *22*, 301–316. [CrossRef]

20. Roy, S.; Senger, K.; Hovland, M.; Römer, M.; Braathen, A. Geological controls on shallow gas distribution and seafloor seepage in an Arctic fjord of Spitsbergen, Norway. *Mar. Pet. Geol.* **2019**, *107*, 237–254. [CrossRef]

21. Roy, S.; Hovland, M.; Braathen, A. Evidence of fl uid seepage in Grønfjorden, Spitsbergen: Implications from an integrated acoustic study of sea floor morphology, marine sediments and tectonics. *Mar. Geol.* **2016**, *380*, 67–78. [CrossRef]

22. Smeaton, C.; Austin, W.E.N.; Davies, A.L.; Baltzer, A.; Howe, J.A.; Baxter, J.M. Scotland's forgotten carbon: A national assessment of mid-latitude fjord sedimentary carbon stocks. *Biogeosciences* **2017**, *14*, 5663–5674. [CrossRef]

23. Smeaton, C.; Austin, W.; Turrell, W. Re-Evaluating Scotlands Sedimentary Carbon Stocks. In *Scottish Marine and Freshwater Science*, 2nd ed.; Marine Scotland: Edinburgh, UK, 2020; Volume 11.

24. Krämer, K.; Holler, P.; Herbst, G.; Bratek, A.; Ahmerkamp, S.; Neumann, A.; Bartholomä, A.; Van Beusekom, J.E.E.; Holtappels, M.; Winter, C. Abrupt emergence of a large pockmark field in the German Bight, southeastern North Sea. *Sci. Rep.* **2017**, *7*, 1–8. [CrossRef]

25. Lohrberg, A.; Schmale, O.; Ostrovsky, I.; Niemann, H.; Held, P.; Deimling, J.S. Von Discovery and quantification of a widespread methane ebullition event in a coastal inlet (Baltic Sea) using a novel sonar strategy. *Sci. Rep.* **2020**, *10*, 1–13. [CrossRef]

26. McGinnis, D.F.; Greinert, J.; Artemov, Y.; Beaubien, S.E.; Wüest, A. Fate of rising methane bubbles in stratified waters: How much methane reaches the atmosphere? *J. Geophys. Res. Ocean.* **2006**, *111*, 1–15. [CrossRef]

27. Smeaton, C.; Hunt, C.A.; Turrell, W.R.; Austin, W.E.N. Marine Sedimentary Carbon Stocks of the United Kingdom's Exclusive Economic Zone. *Front. Earth Sci.* **2021**, *9*, 1–21. [CrossRef]

28. McIntyre, K.L. *Offshore Records of Ice Extent and Deglaciation, Loch Linnhe, Western Scotland*; University of Aberdeen: Aberdeen, UK, 2012.

29. Greene, D. *The Loch Lomond Stadial Ice Cap in Western Lochaber*; University of Edinburgh: Edinburgh, UK, 1995.

30. Stewart, M.; Strachan, R.A.; Holdsworth, R.E. Structure and early kinematic history of the Great Glen Fault Zone, Scotland. *Tectonics* **1999**, *18*, 326–342. [CrossRef]

31. Mcintyre, K.L.; Howe, J.A. Scottish west coast fjords since the last glaciation: A review. *Geol. Soc. Lond. Spec. Publ.* **2010**, *344*, 305–329. [CrossRef]

32. Howe, J.A.; Anderton, R.; Arosio, R.; Dove, D.; Bradwell, T.; Crump, P.; Cooper, R.; Cocuccio, A. The seabed geomorphology and geological structure of the Firth of Lorn, western Scotland, UK, as revealed by multibeam echo-sounder survey. *Earth Environ. Sci. Trans. R. Soc. Edinb.* **2015**, *105*, 273–284. [CrossRef]

33. Golledge, N.R.; Hubbard, A.L.; Sugden, D.E. Mass balance, flow and subglacial processes of a modelled Younger Dryas ice cap in Scotland. *J. Glaciol.* **2009**, *55*, 32–42. [CrossRef]

34. IHO International Hydrographic Organization standards for hydrographic surveys. *Stand. Hydrogr. Surv.* **2020**, *S44*, 51.

35. Gafeira, J.; Dolan, M.; Monteys, X. Geomorphometric characterization of pockmarks by using a GIS-based semi-automated toolbox. *Geosciences* **2018**, *8*, 154. [CrossRef]

36. Moss, J.L.; Cartwright, J.; Cartwright, A.; Moore, R. The spatial pattern and drainage cell characteristics of a pockmark field, Nile Deep Sea Fan. *Mar. Pet. Geol.* **2012**, *35*, 321–336. [CrossRef]

37. Holding, J.M.; Duarte, C.M.; Delgado-Huertas, A.; Soetaert, K.; Vonk, J.E.; Agustí, S.; Wassmann, P.; Middelburg, J.J. Autochthonous and allochthonous contributions of organic carbon to microbial food webs in Svalbard fjords. *Limnol. Oceanogr.* **2017**, *62*, 1307–1323. [CrossRef]

38. Judd, A.; Davies, G.; Wilson, J.; Holmes, R.; Baron, G.; Bryden, I. Contributions to atmospheric methane by natural seepages on the UK continental shelf. *Mar. Geol.* **1997**, *137*, 165–189. [CrossRef]

39. Stoker, M.S.; Bradwell, T.; Howe, J.A.; Wilkinson, I.P.; McIntyre, K. Lateglacial ice-cap dynamics in NW Scotland: Evidence from the fjords of the Summer Isles region. *Quat. Sci. Rev.* **2009**, *28*, 3161–3184. [CrossRef]

40. Stoker, M.; Bradwell, T. Neotectonic deformation in a Scottish fjord, Loch Broom, NW Scotland. *Scottish J. Geol.* **2009**, *45*, 107–116. [CrossRef]

41. Bradwell, T.; Fabel, D.; Clark, C.D.; Chiverrell, R.C.; Small, D.; Smedley, R.K.; Saher, M.H.; Moreton, S.G.; Dove, D.; Callard, S.L.; et al. Pattern, style and timing of British–Irish Ice Sheet advance and retreat over the last 45 000 years: Evidence from NW Scotland and the adjacent continental shelf. *J. Quat. Sci.* **2021**, *36*, 871–933. [CrossRef]

42. Henrichs, S.M.; Reeburgh, W.S. Anaerobic mineralization of marine sediment organic matter: Rates and the role of anaerobic processes in the oceanic carbon economy. *Geomicrobiol. J.* **1987**, *5*, 191–237. [CrossRef]

43. Ingall, E.D.; Cappellen, P. Van Relation between sedimentation rate and burial of organic phosphorus and organic carbon in marine sediments. *Geochim. Cosmochim. Acta* **1990**, *54*, 373–386. [CrossRef]

44. Fader, G.B.J. Gas-related sedimentary features from the eastern Canadian continental shelf. *Cont. Shelf Res.* **1991**, *11*, 1123–1153. [CrossRef]

45. Nørgaard-Pedersen, N.; Austin, W.E.N.; Howe, J.A.; Shimmield, T. The Holocene record of loch etive, western Scotland: Influence of catchment and relative sea level changes. *Mar. Geol.* **2006**, *228*, 55–71. [CrossRef]

46. Svendsen, H.; Beszczynska-Møller, A.; Hagen, J.O.; Lefauconnier, B.; Tverberg, V.; Gerland, S.; Ørbøk, J.B.; Bischof, K.; Papucci, C.; Zajaczkowski, M.; et al. The physical environment of Kongsfjorden-Krossfjorden, and Arctic fjord system in Svalbard. *Polar Res.* **2002**, *21*, 133–166. [CrossRef]

47. Howe, J.A.; Austin, W.E.N.; Forwick, M.; Paetzel, M.; Harland, R.; Cage, A.G. Fjord systems and archives: A review. *Geol. Soc. Lond. Spec. Publ.* **2010**, *344*, 5–15. [CrossRef]

48. Howe, J.A.; Shimmield, T.; Austin, W.E.N.; Longva, O. Post-glacial depositional environments in a mid-high latitude glacially-overdeepened sea loch, inner Loch Etive, western Scotland. *Mar. Geol.* **2002**, *185*, 417–433. [CrossRef]

49. Syvitski, J.P. Water-escape sea floor depressions. In *Glaciated Continental Margins: An Atlas of Acoustic Images*; Davies, T.A., Bell, T., Cooper, A.K., Josenhans, H., Polyak, L., Solheim, A., Stoker, M.S., Stravers, J.A., Eds.; Springer: Dordrecht, The Netherlands, 1997; pp. 160–161. ISBN 978-94-011-5820-6.

50. Roy, S.; Hovland, M.; Noormets, R.; Olaussen, S. Seepage in Isfjorden and its tributary fjords, West Spitsbergen. *Mar. Geol.* **2015**, *363*, 146–159. [CrossRef]

51. Albert, D.B.; Martens, C.S.; Alperin, M.J. Biogeochemical processes controlling methane in gassy coastal sediments—Part 2: Groundwater flow control of acoustic turbidity in Eckernforde Bay Sediments. *Cont. Shelf Res.* **1998**, *18*, 1771–1793. [CrossRef]

52. Cathles, L.M.; Su, Z.; Chen, D. The physics of gas chimney and pockmark formation, with implications for assessment of seafloor hazards and gas sequestration. *Mar. Pet. Geol.* **2010**, *27*, 82–91. [CrossRef]

53. Kennedy, W.Q. The great Glen fault. *Q. J. Geol. Soc.* **1946**, *102*, 41–76. [CrossRef]